EPJ A
Hadrons and Nuclei
www.epj.org

Eur. Phys. J. A **37**, 97–110 (2008) DOI: 10.1140/epja/i2007-10601-5

Correlation and polarization characteristics of the nuclear quasi-free $(\mathrm{p}, \mathrm{d}\pi^+)$ reaction

V.V. Balashov and V.K. Dolinov

EDP SCIENCES
Società Italiana Di Fisica
Springer

Eur. Phys. J. A **37**, 97–110 (2008)
DOI 10.1140/epja/i2007-10601-5

THE EUROPEAN PHYSICAL JOURNAL A

Regular Article – Theoretical Physics

Correlation and polarization characteristics of the nuclear quasi-free $(\mathrm{p}, \mathrm{d}\pi^+)$ reaction

V.V. Balashov[a] and V.K. Dolinov

Institute of Nuclear Physics, Moscow State University, Moscow 119991, Russia

Received: 23 July 2007 / Revised: 20 May 2008
Published online: 20 June 2008 –
Communicated by G. Orlandini

Abstract. An extended set of observables of the nuclear quasi-free $(p, d\pi^+)$ reaction including the triple differential cross-section for coincidence measurements, its analyzing power in case of polarized proton beams and, also, the parameters of the polarization of the excited recoil nucleus and the produced deuteron are considered in the framework of the distorted-wave impulse approximation using the reaction $^{16}\mathrm{O}(\boldsymbol{p}, d\pi^+)^{15}\mathrm{N}$ at a proton energy of 650 MeV as an example. The calculations show a high sensitivity of the differential cross-section and, especially, of the polarization transfer characteristics of the reaction to the spin-multipole decomposition of the amplitude of the basic two-body $pp \to d\pi^+$ process.

PACS. 21.60.Gx Cluster models – 24.50.+g Direct reactions – 24.70.+s Polarization phenomena in reactions – 25.70.Bc Elastic and quasielastic scattering

1 Introduction

The nuclear $(p, d\,\pi^+)$ reaction is of interest for extended experimental and theoretical studies as an example of specific quasi-free cluster composing processes where, contrary to the well-known $(p, p\,d)$ reaction [1–4], the deuteron is not knocked-out from a nucleus under quasi-elastic proton scattering from the deuteron cluster, but is formed together with the pion in the two-body proton-proton collision $pp \to d\pi^+$.

The quasi-free character of the nuclear $(p, d\,\pi^+)$ reaction was demonstrated in Dubna in 1970 in the course of the investigation of the interaction of 670 MeV protons with the $^{12}\mathrm{C}$ target [5]. The kinematic analysis of two characteristic bumps in the deuteron energy distribution has pointed out to their clear correspondence to the forward-angle and back-angle deuteron production in the center-of-mass frame of the two-body $pp \to d\pi^+$ process. The contribution of this mechanism to the deuteron yield was shown to prevail over that from the deuteron quasi-elastic knock-out reaction $p + d \to p + d$. These results opened a way to theoretical investigations in the field [6,7] including a first estimate of the advantages [6] expected to come from coincidence deuteron-pion measurements. The possibility to obtain information on the population of excited states of the recoil nucleus in the $(p, d\pi^+)$ reaction was one of them.

First coincidence $(p, d\pi^+)$ measurements were performed two decades later at Stellenbosch with the reaction $^{12}\mathrm{C}(p, d\pi^+)^{11}\mathrm{B}_{g.s.}$ [8]. In spite of the rather low energy of the proton beam used in these experiments (which was even below the $pp \to d\pi^+$ threshold on a free proton at rest), the measurement results and their theoretical analysis in the same paper have led to an unambiguous conclusion about the quasi-free nature of the reaction observed. The present-day level of experimental and theoretical studies on the quasi-free process $(p, d\pi^+)$ is demonstrated by paper [9] devoted to the nuclear reaction $^{12}\mathrm{C}(\boldsymbol{p}, d\pi^+)^{11}\mathrm{B}$. Much higher proton energies (370 and 500 MeV against 223 MeV in paper [8]), a good energy resolution which makes possible to separate the reaction channels corresponding to the ground and to low-lying excited states of the recoil nucleus, a set of different combinations of the deuteron and pion detection angles, and using a polarized incoming proton beam —all these experimental advantages of the studies [9] were enforced by a scrupulous theoretical analysis of the measurement results performed in this paper within PWIA and DWIA versions of the impulse approximation. To obtain and analyze the differential cross-sections and the analyzing power not only for the recoil nucleus ground state but also, at the same level, for its excited states was one of the main goals of the work [9]. Here, in comparison between experimental results and calculations, a number of open questions remained. They led the authors of paper [9] (part VI, right side) to conclude that another case, the re-

[a] e-mail: balvse@anna19.sinp.msu.ru

action $^{16}\mathrm{O}(p, d\pi^+)^{15}\mathrm{N}$, could be more interesting than the reaction $^{12}\mathrm{C}(p, d\pi^+)^{11}\mathrm{B}$ for further investigation of the general features of the quasi-free $(p, d\pi^+)$ process. This conclusion became a starting point for our own study. Besides, one cannot miss one important result of the measurements [9] which was not discussed in that paper. We mean a remarkable difference in the profile of the pion energy dependence of the differential cross-sections of the reaction to the ground state of the recoil nucleus and to its excited state $^{11}\mathrm{B}^*(3/2^-; 5.02\,\mathrm{MeV})$. All angular momenta and parity quantum numbers are identical in these two channels corresponding to the case of the collision of the bombarding proton with a nuclear proton in the same $1p_{3/2}$ shell. According to basic concepts of the quasi-free approach, their differential cross-sections must be proportional to their spectroscopic factors, with no more difference between them. Observed purely experimentally, the violation of this criterium in the reaction $^{12}\mathrm{C}(p, d\pi^+)^{11}\mathrm{B}$ is highly significant.

Our general approach to consider the differential cross-section $\mathrm{d}^3\sigma/\mathrm{d}\Omega_d\mathrm{d}\Omega_\pi\mathrm{d}T_\pi$ and the analyzing power $\mathcal{A}_{\boldsymbol{p},\pi d}$ for the $(\boldsymbol{p}, d\pi^+)$ reaction is outlined in sect. 2. To stress the quasi-free character of the reaction under consideration, it is interesting to go to a higher energy of the incoming proton than in papers [8,9]. Two sources [10,11] are well known to parameterize the amplitude of the free two-body reaction $pp \to d\pi^+$. We take the same Bugg systematization as in paper [9] and perform our calculation for the incoming proton energy $T_p = 650\,\mathrm{MeV}$, which corresponds to the upper limit of data available in [10]. All our calculations are made within the distorted-wave DWIA approach compared, in some cases, with the simplified PWIA one to show the role of the initial- and final-state proton, deuteron and pion interactions with the nucleus. The orientation to higher energies of the proton beam makes it possible to simplify the procedure to calculate the distorted-wave functions of the projectile and produced particles and to use, instead of the partial-wave expansion approach of paper [9], the eikonal (Glauber) method, increasingly used in recent theoretical calculations on the quasi-free processes [12,13]. When calculating the differential cross-section $\mathrm{d}^3\sigma/\mathrm{d}\Omega_d\mathrm{d}\Omega_\pi\mathrm{d}T_\pi$, we do not factorize it to the two-body $pp \to d\pi^+$ cross-section and nuclear form factor (such an approximation, in spite of the rather high energy of our proton, would be too rough in this case).

In sect. 3 we present our results for the differential cross-section and analyzing power of the reaction $^{16}\mathrm{O}(\boldsymbol{p}, d\pi^+)^{15}\mathrm{N}$ in its two channels $^{16}\mathrm{O} \to {}^{15}\mathrm{N}(1p^{-1}_{1/2})$ and $^{16}\mathrm{O} \to {}^{15}\mathrm{N}(1p^{-1}_{3/2})$. The polarization of the recoil nucleus and produced deuteron is considered in sect. 4. A special attention is given to the concept of effective (orbital) polarization of the target proton induced by the initial-state and final-state particle-nucleus interactions. We show that its applicability is limited by the spin-orbit effects in the distortion of the wave functions of the incoming proton and, especially, of the produced deuteron. As a fact, all the characteristics of the reaction taken for consideration —from the differential cross-section of the reaction with non-polarized protons to the proton-to-deuteron polarization transfer parameters— are calculated without using the effective polarization concept. Nevertheless, a number of parallel calculations of the same characteristics are performed using this concept to show that, depending on the conditions taken, it can either be working well or turns out to be invalid. To investigate the sensitivity of the observables of the $(\boldsymbol{p}, d\pi^+)$ reaction to the parametrization of the amplitude of the elementary two-body $pp \to d\pi^+$ process is another important goal of our work.

The *Madison convention* [14] to choose the coordinate frame and quantization axis is used throughout this work.

2 The $(\mathbf{p}, \mathrm{d}\pi^+)$ reaction in the DWIA approach

2.1 Reaction amplitude, differential cross-section, analyzing power

Consider the differential cross-section for the $(\boldsymbol{p}, d\pi^+)$ reaction from a zero-spin nucleus where the pion and the deuteron are produced with momenta $\boldsymbol{k}_\pi$ and $\boldsymbol{k}_d$ under the condition that the recoil nucleus remains in a fixed state $|J_R\rangle$ with its total angular momentum J_R. Suppose, to begin, that no polarization parameters of the incoming proton and of both the recoil nucleus and the produced deuteron are detected. The equation

$$\frac{\mathrm{d}^3\sigma_{J_R}}{\mathrm{d}\Omega_\pi\mathrm{d}\Omega_d\mathrm{d}T_\pi}(\boldsymbol{k}_\pi, \boldsymbol{k}_d; \boldsymbol{k}_p) = \frac{1}{2} \times \sum_{\mu_p,\mu_d,M_R} \left|\langle J_R, M_R; \boldsymbol{k}_\pi, \boldsymbol{k}_d, \mu_d|\hat{F}|\boldsymbol{k}_p, \mu_p\rangle\right|^2 \quad (1)$$

with $\boldsymbol{k}_p$ standing for the momentum of the incoming proton, where the sum is taken over magnetic quantum numbers μ_p, μ_d and M_R of the proton, the deuteron and the recoil nucleus, connects this differential cross-section with the reaction amplitude $\langle J_R, M_R; \boldsymbol{k}_\pi, \boldsymbol{k}_d, \mu_d|\hat{F}|\boldsymbol{k}_p, \mu_p\rangle$. Within the DWIA approximation, the latter is calculated using the amplitude $\langle \boldsymbol{K}_{\pi d}, \mu_d|\hat{t}(E^{c.m.}_{pp'\to d\pi^+})|\boldsymbol{K}_{pp'}, \mu_p, \mu_{p'}\rangle$ of the two-body free process $pp \to d\pi^+$

$$\langle J_R, M_R; \boldsymbol{k}_\pi, \boldsymbol{k}_d, \mu_d|\hat{F}|\boldsymbol{k}_p, \mu_p\rangle = (\mathcal{K}_{lab}N_T)^{1/2} \times \sum_{\mu_{p'}} \langle \boldsymbol{K}_{\pi d}, \mu_d|\hat{t}(E^{c.m.}_{pp'\to d\pi^+})|\boldsymbol{K}_{pp'}, \mu_p, \mu_{p'}\rangle \times \mathcal{F}(J_R, M_R, \mu_{p'}; \boldsymbol{k}_\pi, \boldsymbol{k}_d, \boldsymbol{k}_p), \quad (2)$$

where $E^{c.m.}_{pp'\to d\pi^+}$, $\boldsymbol{K}_{pp'}$ and $\boldsymbol{K}_{\pi d}$ are the total energy and momenta of the corresponding pairs of particles in their center-of-mass frame.

Usually, the nuclear matrix element

$$\mathcal{F}(J_R, M_R, \mu_{p'}; \boldsymbol{k}_\pi, \boldsymbol{k}_d, \boldsymbol{k}_p) = c_{J_R}\frac{(-1)^{l+s_p-M_R}}{\sqrt{2J_R+1}} \times \sum_{m_l} (lm_l, s_p\mu_{p'}|J_R, -M_R) H_{nlm_l}(\boldsymbol{k}_\pi, \boldsymbol{k}_d, \boldsymbol{k}_p) \quad (3)$$

is reduced to a simple overlap integral

$$H_{nlm_l}(\boldsymbol{k}_\pi, \boldsymbol{k}_d, \boldsymbol{k}_p) = (2\pi)^{-3/2} \times \int e^{i\boldsymbol{k}_R \boldsymbol{r}} \varPhi_{nlm_l}(\boldsymbol{r}) \left[D^{(-)}_{\boldsymbol{k}_d}(\boldsymbol{r}) D^{(-)}_{\boldsymbol{k}_\pi}(\boldsymbol{r}) \right]^* D^{(+)}_{\boldsymbol{k}_p}(\boldsymbol{r}) \mathrm{d}^3 r \quad (4)$$

of the target proton wave function $\varPhi_{nlm_l}(\boldsymbol{r})$ and distorted-wave functions of the incoming proton and two produced particles. Strictly speaking, the former should be calculated separately for each of the reaction channels taking into account the proton binding energy difference between them. The calculation shows, however, that this effect is negligibly small in our case. For the same reason, we believe that the wave functions of the remaining part of the target nucleons overlap completely with those in the recoil nucleus. As for the distorted waves, we calculate them within the eikonal approximation

$$\psi_{\boldsymbol{k}_p}(\boldsymbol{r}) = e^{i\boldsymbol{k}_p \boldsymbol{r}} D^{(+)}_{\boldsymbol{k}_p}(\boldsymbol{r});$$
$$D^{(+)}_{\boldsymbol{k}_p}(\boldsymbol{r}) = \exp\left(-\frac{i}{\beta_p} \int_0^\infty V_p\left(\boldsymbol{r} - \frac{\boldsymbol{k}_p}{k_p} s \right) \mathrm{d}s \right), \quad (5)$$

where β_p and

$$\boldsymbol{k}_R = \boldsymbol{k}_p - \boldsymbol{k}_d - \boldsymbol{k}_\pi$$

stand for the velocity of the corresponding particles and the recoil nucleus momentum. Equation (2) also contains: a kinematic factor

$$\mathcal{K}_{lab} = \frac{k_\pi k_d}{k_p} \cdot \frac{k_p^*}{k_\pi^*} (E_\pi^* + E_d^*) \frac{E_p^* + E_{p'}^*}{E_{p'}^*} \times \frac{E_p}{E_p^*} \frac{E_\pi}{E_\pi^*} \frac{E_d}{E_d^*} \left| 1 - \boldsymbol{\beta}_d \boldsymbol{\beta}_R / \beta_d^2 \right|^{-1}$$

(given here in the lab frame); the total energies E_i, E_i^* of the particle i in the lab frame and in the center-of-mass frame of the two-body process $pp \to d\pi^+$; the total number of protons N_T in the nuclear shell taking part in the reaction; the fraction parentage coefficient c_{J_R} for the overlap degree between the wave function of the target nucleus in its ground state and that of the recoil nucleus in the corresponding reaction channel. The latter, together with N_T, is leading to the spectroscopic factor S_{J_R} of the reaction

$$S_{J_R} = N_T |c_{J_R}|^2 \,.$$

The formulae above disregard spin-dependent interactions in the initial and final states of the reaction. When taking these interactions into account and inserting the spin-orbit component $V_p^{(ls)}(\boldsymbol{r}) = \alpha_{ls}(r) \boldsymbol{L}_p \boldsymbol{S}_p$ into the optical potentials $\hat{V}_p(\boldsymbol{r}) = V_p^{(c)}(r) + V_p^{(ls)}(\boldsymbol{r})$ of the incoming proton and the produced deuteron, we extend this formalism and treat the distortion factors $D^{(+)}_{\boldsymbol{k}_p}(\boldsymbol{r})$ and $D^{(-)}_{\boldsymbol{k}_d}(\boldsymbol{r})$ of both particles as matrices $\hat{D}^{(\pm)}_{\boldsymbol{k}}(\boldsymbol{r})$ over the magnetic quantum numbers of their spin. Together with them, the integral (4) is transformed into a direct product $\hat{H}_{nlm_l}(\boldsymbol{k}_\pi, \boldsymbol{k}_d, \boldsymbol{k}_p)$ of corresponding 2×2 and 3×3 spin matrices.

The matrix elements of the generalized distortion factors are calculated as

$$\langle \mu | \hat{D}_p(\boldsymbol{k}_p; \boldsymbol{r}) | \nu \rangle = \phi_\nu^{(\mu)}(\boldsymbol{r})$$

by using the auxiliary functions $\phi_\nu^{(\mu)}(\boldsymbol{r})$ satisfying a system of differential equations

$$i \frac{\partial \phi_\nu^{(\mu)}(\boldsymbol{b}, z)}{\partial z} = \frac{1}{\beta_p} \sum_{\nu'} \langle \nu | \hat{V}_p(\boldsymbol{b}, z) | \nu' \rangle \phi_{\nu'}^{(\mu)}(\boldsymbol{b}, z). \quad (6)$$

They are solved approximately by substituting the kinematically determined proton or deuteron momenta $\boldsymbol{k}_p$, $\boldsymbol{k}_d$ into the angular-momentum operator $\hat{\boldsymbol{L}} = [\hat{\boldsymbol{r}} \times \hat{\boldsymbol{p}}]$ of the corresponding particle instead of the operator $\hat{\boldsymbol{p}} = -i\hbar\hat{\nabla}$ of its momentum.

In calculating the proton distortion factor $\hat{D}_p^{(+)}(\boldsymbol{k}_p; \boldsymbol{r})$ these equations are solved under the condition

$$\phi_{\nu_p}^{(\mu_p)}(\boldsymbol{b}, z = -\infty) = \delta_{\mu_p, \nu_p} \,,$$

where μ_p, ν_p stands for the spin orientation quantum numbers of the proton. Using the time reversal relation

$$D^{(-)}_{\boldsymbol{k}_d}(\boldsymbol{r}) = D^{(+)}_{-\boldsymbol{k}_d}(\boldsymbol{r})^* \,,$$

equations of the same form are used to obtain the spin matrix $\hat{D}_d^{(-)}(\boldsymbol{k}_d; \boldsymbol{r})$ for the deuteron distortion factor. Here, the procedure consists of two steps. First, we follow (6) to calculate the matrix $\langle \mu_d | \hat{D}_d^{(-)}(\boldsymbol{k}_d; \boldsymbol{r}') | \nu_d \rangle$ in the coordinate frame $\boldsymbol{r}' = (\boldsymbol{b}', z')$ with the quantization axis z along the deuteron momentum $\boldsymbol{k}_d$. Then, using Wigner spin rotation matrices $D^{(S_d=1)}_{\mu\mu'}(\boldsymbol{k}_d \to \boldsymbol{k}_p)$, it is transformed into the laboratory coordinate frame with the axis z along the incoming proton momentum $\boldsymbol{k}_p$.

According to general rules to deal with off-energy-shell effects in nuclear quasi-free processes, the relative momenta $\boldsymbol{K}_{pp'}$, $\boldsymbol{K}_{\pi d}$ of the two colliding protons and of the produced pion-deuteron pair as well as their total energy $E^{c.m.}_{pp' \to d\pi^+}$ in the center-of-mass frame can be calculated using the *initial energy prescription* or the *final energy prescription* (see, *e.g.*, [8]). But the calculation shows that the difference between these two variants is very small at our energy $T_p = 650\,\mathrm{MeV}$.

Equation (1) is reduced to a simpler one within the *factorization approximation* [15]. Here the differential cross-section is calculated as

$$\frac{\mathrm{d}^3 \sigma_{J_R}}{\mathrm{d}\Omega_\pi \mathrm{d}\Omega_d \mathrm{d}T_\pi}(\boldsymbol{k}_\pi, \boldsymbol{k}_d; \boldsymbol{k}_p) = \mathcal{K}_{lab} \left(\frac{\mathrm{d}\sigma}{\mathrm{d}\Omega_\pi} \right)^{(c.m.)} \times W_{J_R}(\boldsymbol{k}_\pi, \boldsymbol{k}_d; \boldsymbol{k}_p), \quad (7)$$

where

$$\left(\frac{\mathrm{d}\sigma}{\mathrm{d}\Omega_\pi} \right)^{c.m.} = \frac{1}{(2s_p + 1)(2s_{p'} + 1)} \times \sum_{\mu_p \mu_{p'} \mu_d} \left| \langle \boldsymbol{K}_{\pi d}, \mu_d | \hat{t}(E^{c.m.}_{pp' \to d\pi^+}) | \boldsymbol{K}_{pp'}, \mu_p, \mu_{p'} \rangle \right|^2$$

stands for the differential cross-section of the free two-body process $pp \to d\pi^+$ in the center-of-mass frame of the interacting particles while the *distorted momentum distribution* of the target proton

$$W_{J_R}(\boldsymbol{k}_\pi, \boldsymbol{k}_d; \boldsymbol{k}_p) = N_T \sum_{M_R \mu_{p'}} |\mathcal{F}(J_R, M_R, \mu_{p'}; \boldsymbol{k}_\pi, \boldsymbol{k}_d, \boldsymbol{k}_p)|^2 = \frac{S_{J_R}}{2l+1} \sum_{m_l} |H_{nlm_l}(\boldsymbol{k}_\pi, \boldsymbol{k}_d; \boldsymbol{k}_p)|^2$$

enters the equation as a nuclear form factor. Within the PWIA approach it is transformed into the momentum distribution $|\Phi_{nl}(\boldsymbol{k}_R)|^2$ of the target proton.

For the $(\boldsymbol{p}, d\pi^+)$ reaction with polarized protons, we introduce the analyzing power of the differential cross-section (1) in its standard form

$$\mathcal{A}_0(\boldsymbol{k}_\pi, \boldsymbol{k}_d | \boldsymbol{k}_p) = \frac{\mathrm{d}^3\sigma_{J_R}^{(up)} - \mathrm{d}^3\sigma_{J_R}^{(down)}}{\mathrm{d}^3\sigma_{J_R}^{(up)} + \mathrm{d}^3\sigma_{J_R}^{(down)}}\,, \tag{8}$$

where $\mathrm{d}^3\sigma_{J_R}^{(up/down)}$ stands for the cross-sections for protons totally polarized "up" ($\mu_p = 1/2$) or "down" ($\mu_p = -1/2$) along the normal $\boldsymbol{n}$ to the reaction plane. They can be calculated using eq. (1) when summation over the magnetic quantum number μ_p of the incoming proton is excluded from this formula. According to the *Madison convention* [14], the axis z is directed along the incoming proton momentum $\boldsymbol{k}_p$; the axis y is perpendicular to the reaction plane and directed along the vector product $\boldsymbol{n} \sim [\boldsymbol{k}_p \times \boldsymbol{k}_\pi]$ of the momenta of the incoming proton and produced pion; so, the axis x lies in the reaction plane.

2.2 Amplitude of the free two-body process pp → dπ⁺

With usual angular-momentum algebra, one decomposes the two-body $pp \to d\pi^+$ amplitude (2) into a superposition of the partial amplitudes $\langle L_{\pi d}|t_J(E^{c.m.}_{pp' \to d\pi^+})|L_{pp'} S_{pp'}\rangle$

$$\langle \boldsymbol{K}_{\pi d}, \mu_d | \hat{t} | \boldsymbol{K}_{pp'}, \mu_p, \mu_{p'}\rangle = \sum_{L_{\pi d} L_{pp'} S_{pp'} J} c_J(\boldsymbol{K}_{\pi d}, \mu_d, L_{\pi d}; \boldsymbol{K}_{pp'}, \mu_p, \mu_{p'}, L_{pp'}, S_{pp'}) \times \sqrt{\frac{4\pi}{2L_{pp'}+1}} \langle L_{\pi d}|t_J(E^{c.m.}_{pp' \to d\pi^+})|L_{pp'}, S_{pp'}\rangle, \tag{9}$$

$$c_J(\boldsymbol{K}_{\pi d}, \mu_d, L_{\pi d}; \boldsymbol{K}_{pp'}, \mu_p, \mu_{p'}, L_{pp'}, S_{pp'}) = \sum_{M_{\pi d}, M_{pp'}} (s_p\mu_p, s_p\mu_{p'}|S_{pp'}\sigma_{pp'})(L_{\pi d}M_{\pi d}, s_d\mu_d|JM) \times (L_{pp'}M_{pp'}, S_{pp'}\sigma_{pp'}|JM) Y_{L_{\pi d}M_{\pi d}}(\hat{K}_{\pi d}) Y^*_{L_{pp'}M_{pp'}}(\hat{K}_{pp'}),$$

where $L_{pp'}$ and $L_{\pi d}$ are the relative orbital momenta of the corresponding pairs of particles in the initial and final states and $S_{pp'}$ is the summed spin of the two colliding protons. The widely used notation by Mandle and Regge [16] for the first seven amplitudes $a_0, \ldots, a_6$ is given in table 1.

Table 1. Nomenclature [16] for the partial amplitudes $\langle L_{\pi d}|t_J(E^{c.m.}_{pp' \to d\pi^+})|L_{pp'}, S_{pp'}\rangle$.

Amplitude	$S_{pp'}$	$L_{pp'}$	$L_{\pi d}$	J
a_0	0	0	1	0
a_1	1	1	0	1
a_2	0	2	1	2
a_3	1	1	2	1
a_4	1	1	2	2
a_5	1	3	2	2
a_6	1	3	2	3

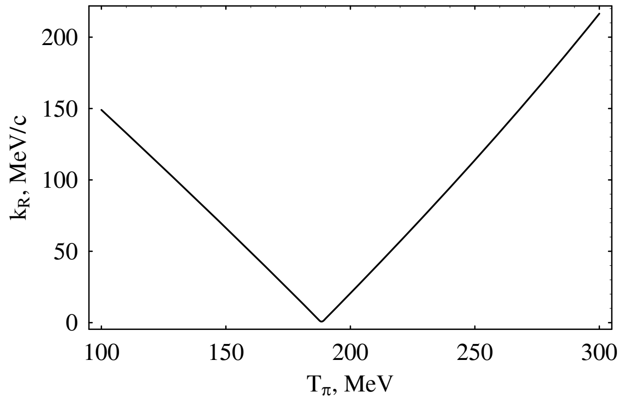

Fig. 1. Momentum k_R of the recoil nucleus in the reaction $^{16}\mathrm{O}(\boldsymbol{p}, d\pi^+)^{15}\mathrm{N}_{g.s.}$ as a function of pion kinetic energy T_π (both k_R and T_π in the lab frame) under conditions (10).

3 Reaction ¹⁶O(p, dπ⁺)¹⁵N: differential cross-section and analyzing power

3.1 Kinematic and geometry conditions; input parameters for the calculation

Following [9], consider a coplanar case of the $(p, d\pi^+)$ reaction. In the quasi-free process, the maximal intensity of the πd coincidence events corresponds to the region of small values $k_{p'}$ of the target proton momentum (in light $1p$-shell nuclei, near $180\,\mathrm{MeV}/c$). Throughout this paper we fix the incoming proton energy, the polar and azimuthal escape angles of the produced pion and deuteron as

$$T_p = 650\,\mathrm{MeV}; \quad \theta_\pi^{lab} = 52°; \quad \theta_d^{lab} = 12°; \quad \phi_\pi^{lab} = 0; \quad \phi_d^{lab} = 180°\,. \tag{10}$$

Then, in each of the reaction channels $^{16}\mathrm{O} \to {}^{15}\mathrm{N}(1p_{1/2}^{-1})$ and $^{16}\mathrm{O} \to {}^{15}\mathrm{N}(1p_{3/2}^{-1})$, the kinetic energy T_i^{lab} of any particle in the final state of the reaction determines all other kinematic variables of the reaction in both lab and center-of-mass frames. Figure 1 shows the momentum k_R of the recoil nucleus $^{15}\mathrm{N}$ as a function of kinetic energy T_π of the produced pion under conditions (10). At $T_\pi = 188\,\mathrm{MeV}$, the recoil momentum k_R is zero. The differential cross-section of the reaction under consideration is localized mainly in the T_π region from 100 to 300 MeV. In this range the kinetic energy T_d^{lab} of the deuteron falls linearly with T_π from 400 MeV to 200 MeV, while the momentum $K_{\pi d}$ of the πd pair in their center-of-mass frame is rising (also practically linearly) from 165 MeV/c up to 315 MeV/c. In this frame, the pion escape angle is practically constant in the whole range: $\theta_\pi^{c.m.} \approx 85°$.

We use standard Woods-Saxon parameters $V_0 = 50$ MeV, $R = 2.9$ fm and $a = 0.7$ fm to calculate the wave function of the target proton. The optical potential $\hat{V}_p(r)$ for the incoming proton is obtained by transformation of the Dirac equation optical potential [17] into the Schödinger equation form. The parameters of the deuteron-nucleus interaction $V_d(r)$ including its spin-orbit part were obtained by interpolation of those from work [18] for the elastic scattering of polarized deuterons from the ^{16}O nucleus at 200, 400 and 700 MeV. The Rayligh-Lax form

$$V_\pi(r) = -\frac{i}{2}\beta_\pi \sigma_{\pi N}(1 - i\alpha_{\pi N})\rho_N(r),$$

with the resonance pion-nucleon cross-section

$$\sigma_{\pi N}(k_\pi^{c.m.}) = \sigma_{\pi N}^0 \frac{(\frac{\Gamma_\Delta[\rho_N(r)]}{2})^2}{(M(k_\pi^{c.m.}) - M_\Delta)^2 + (\frac{\Gamma_\Delta[\rho_N(r)]}{2})^2} + \sigma_{bgr} \tag{11}$$

to take into account the Δ-isobar formation, is used for the pion-nucleus optical potential where $M(k_\pi^{c.m.})$ is the effective mass of the πN pair. The nuclear density dependence of the decay width $\Gamma_\Delta[\rho_N(r)]$ of the Δ-isobar comes from taking into account its two-nucleon annihilation channel $N\Delta \to NN$ in nuclear matter. We introduce this correction within the local density approximation to the self-energy Σ_Δ of the Δ-isobar

$$\Gamma_\Delta[\rho_N(r)] = \Gamma_\Delta^{(free)} - 2\,\mathrm{Im}\,\Sigma_\Delta[\rho_N(r)]$$

following its parametrization in [19]. The numerical values $\sigma_{\pi N}^0 = 200$ mb, $M_\Delta = 1232$ MeV, $\Gamma_\Delta^{(free)} = 115$ MeV, $\sigma_{bgr} = 10$ mb, $\alpha_{\pi N} = 0$ for the other parameters are taken from [20].

3.2 Differential cross-sections and the analyzing power in channels ^{16}O $\to$ ^{15}N($1p_{1/2}^{-1}$) and ^{16}O $\to$ ^{15}N($1p_{3/2}^{-1}$)

The calculated differential cross-sections for a case of non-polarized incoming protons are shown in fig. 2 in solid lines. The results for the two reaction channels ^{16}O $\to$ ^{15}N($1p_{1/2}^{-1}$) and ^{16}O $\to$ ^{15}N($1p_{3/2}^{-1}$) differ from each other insignificantly: their T_π-dependence is practically the same while their ratio 1:2 is not more than the statistical weight ratio for the corresponding ($1p_{1/2}^{-1}$) and ($1p_{3/2}^{-1}$) states of the recoil nucleus. The figures show also that the factorization approximation (dashed lines) leads practically to the same results as obtained without this approximation.

Another situation takes place concerning the analyzing power $\mathcal{A}_0(T_\pi)$. Its T_π-dependence is different in the

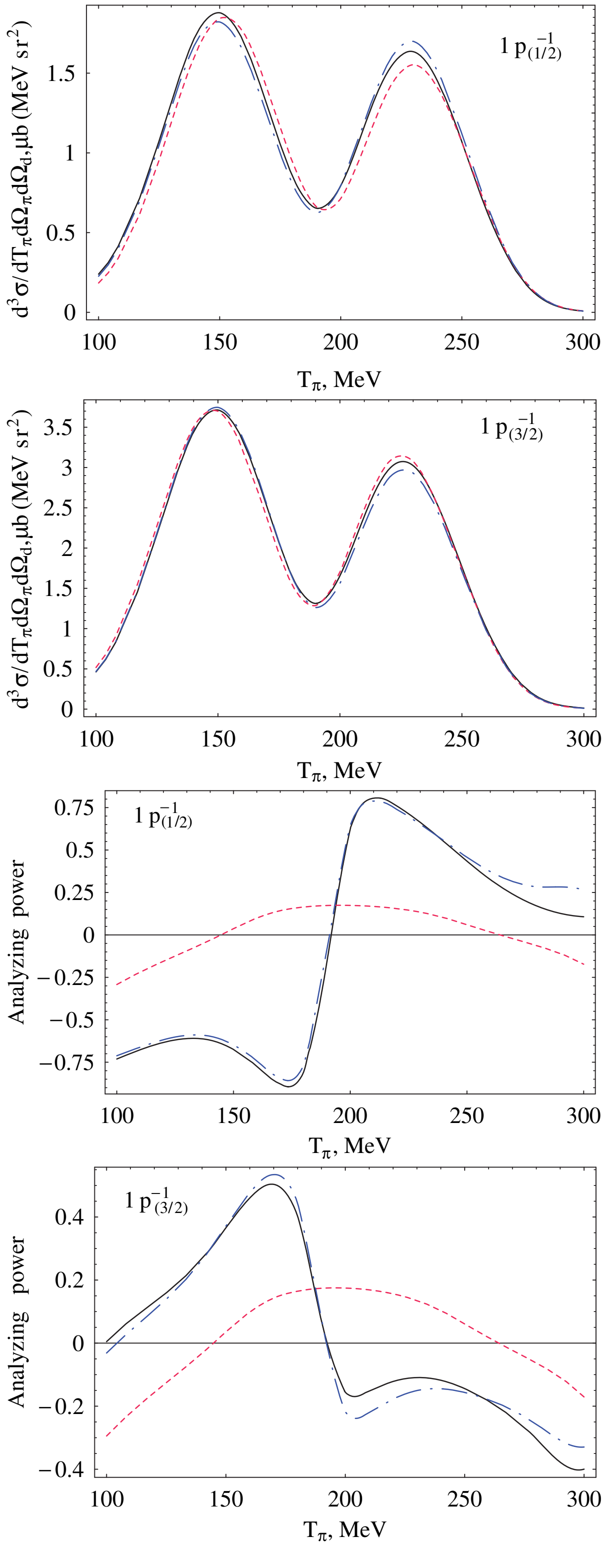

Fig. 2. Differential cross-section and analyzing power $\mathcal{A}_0(\boldsymbol{k}_\pi, \boldsymbol{k}_d|\boldsymbol{k}_p)$ for the reaction ^{16}O$(p, d\pi^+)^{15}$N in the ^{16}O $\to$ ^{15}N($1p_{1/2}^{-1}$) and ^{16}O $\to$ ^{15}N($1p_{3/2}^{-1}$) channels as a function of the pion kinetic energy T_π in the lab frame calculated with the spin-orbit term in the proton and deuteron optical potentials taken (solid lines) and not taken (dash-dotted lines) into account; dashed lines —the same as in solid lines but calculated within the factorization approximation (7).

channels $^{16}\mathrm{O} \to {}^{15}\mathrm{N}(1p^{-1}_{1/2})$ and $^{16}\mathrm{O} \to {}^{15}\mathrm{N}(1p^{-1}_{3/2})$, while the range of variation of its value with T_π is much wider in the first case in comparison to the second one. The analyzing power calculated without the factorization approximation differs considerably from that obtained within this approximation. In the latter case the analyzing power $\mathcal{A}_0(T_\pi)$ for the reaction $^{16}\mathrm{O}(\boldsymbol{p}, d\pi^+)^{15}\mathrm{N}$ is reduced to that in the elementary two-body $pp \to d\pi^+$ process and is the same in both reaction channels $^{16}\mathrm{O} \to {}^{15}\mathrm{N}(1p^{-1}_{1/2})$ and $^{16}\mathrm{O} \to {}^{15}\mathrm{N}(1p^{-1}_{3/2})$ within the DWIA as well as within the PWIA approach.

The dash-dotted lines in fig. 2 correspond to the DWIA calculations similar to those shown by solid lines but simplified by ignoring the spin-orbit term in the optical potentials of the proton-nucleus and deuteron-nucleus interaction in the initial and final states of the reaction. The comparison of these calculations confirms expectations in [9] that the final-state spin-orbit deuteron-nucleus interactions can be of negligibly small influence on the differential cross-section of the $(p, d\pi^+)$ reaction with unpolarized protons as well as on its initial-state spin observables in case of polarized protons such as the analyzing power of the reaction.

The role of the Δ-isobar formation in the final state of the reaction is another important aspect of the problem of the influence of the distortion of the proton, deuteron and pion wave functions by their interaction with the nucleus on the reaction observables. Figure 3 shows that a strong modification of the pion-nucleus interaction in the nuclear matter due to the Δ-isobar formation leads not only to some damping of the pion production but also to nontrivial transformation of the T_π profile of the analyzing power of the reaction.

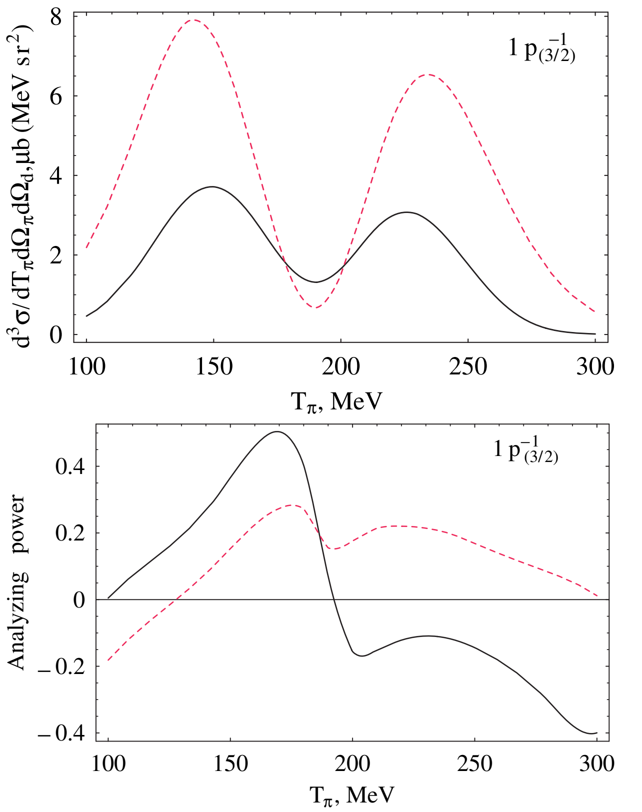

Fig. 3. Differential cross-section and analyzing power $\mathcal{A}_0(\boldsymbol{k}_\pi, \boldsymbol{k}_d|\boldsymbol{k}_p)$ for the $^{16}\mathrm{O}(\boldsymbol{p}, d\pi^+)^{15}\mathrm{N}(1p^{-1}_{3/2})$ reaction calculated taking into account (solid lines) and ignoring (dashed lines) the first (resonance) term in the pion-nucleus cross-section (11).

3.3 Effective polarization of the nuclear proton

The concept of effective (orbital) polarization of the nuclear proton in direct quasi-free processes is well known in physics of the quasi-elastic $(p, 2p)$ reaction [21–23]. In paper [9] it was used to treat the $(p, d\pi^+)$ reaction. The observation of a small influence of the spin-orbit distorting interactions on the differential cross-section and the analyzing power of the reaction was made in the preceding subsection. On this ground and continuing the line of paper [9] one can introduce a simplified concept of the effective orbital polarization of the target proton by ignoring the spin-orbit distortion effects in the initial and final states of the reaction with the purpose to use it, at least, in calculating reaction observables averaged over the orientation of the spin of the produced deuteron. We shall operate with the parameter $P_{eff}(\boldsymbol{k}_p; \boldsymbol{k}_\pi, \boldsymbol{k}_d)$ of the effective orbital polarization in the $(p, d\pi^+)$ reaction when all three momenta $\boldsymbol{k}_p$, $\boldsymbol{k}_\pi$ and $\boldsymbol{k}_d$ lie in one plane (the coplanar geometry). In our case of the $1p$-shell target nucleus this reads

$$P_{eff}(\boldsymbol{k}_p; \boldsymbol{k}_\pi, \boldsymbol{k}_d) = \frac{|H_{1p,m_l=1}(\boldsymbol{k}_p; \boldsymbol{k}_\pi, \boldsymbol{k}_d)|^2 - |H_{1p,m_l=-1}(\boldsymbol{k}_p; \boldsymbol{k}_\pi, \boldsymbol{k}_d)|^2}{|H_{1p,m_l=1}(\boldsymbol{k}_p; \boldsymbol{k}_\pi, \boldsymbol{k}_d)|^2 + |H_{1p,m_l=-1}(\boldsymbol{k}_p; \boldsymbol{k}_\pi, \boldsymbol{k}_d)|^2}, \quad (12)$$

where the nuclear matrix elements $H_{1p,m_l=\pm1}(\boldsymbol{k}_p; \boldsymbol{k}_\pi, \boldsymbol{k}_d)$ with $m_l = \pm1$ are calculated according to the simple equation (4) with projection $m_l = \pm1$ of the proton orbital momentum taken on the normal to the reaction plane.

This parameter can serve as a measure of combined influence of the initial-state and final-state particle-nucleus interactions on the reaction observables. It disappears in the PWIA case. In the DWIA calculations, its magnitude and its T_π profile depend mainly on the imaginary part of the corresponding optical potentials (see fig. 4). It is of practical use to note that $P_{eff}(\boldsymbol{k}_p; \boldsymbol{k}_\pi, \boldsymbol{k}_d)$ shows the degree of deviation of the analyzing power of the differential cross-section for the $(\boldsymbol{p}, d\pi^+)$ *nuclear reaction* from that for the *free two-body process* $pp \to d\pi^+$. In our case of the reaction $^{16}\mathrm{O}(p, d\pi^+)^{15}\mathrm{N}$, their interrelation is demonstrated by equations

$$\mathcal{A}_0^{(1p^{-1}_{1/2})}(\boldsymbol{k}_\pi, \boldsymbol{k}_d|\boldsymbol{k}_p) = \frac{A_{beam} - P_{eff}C_{correl}}{1 - P_{eff}A_{target}}, \quad (13)$$

$$\mathcal{A}_0^{(1p^{-1}_{3/2})}(\boldsymbol{k}_\pi, \boldsymbol{k}_d|\boldsymbol{k}_p) = \frac{A_{beam} + \frac{1}{2}P_{eff}C_{correl}}{1 + \frac{1}{2}P_{eff}A_{target}} \quad (14)$$

for both reaction channels $^{16}\mathrm{O} \to {}^{15}\mathrm{N}(1p^{-1}_{1/2})$ and $^{16}\mathrm{O} \to {}^{15}\mathrm{N}(1p^{-1}_{3/2})$. Here A_{beam}, A_{target} and C_{correl} are the analyzing power and proton spin correlation parameters in the

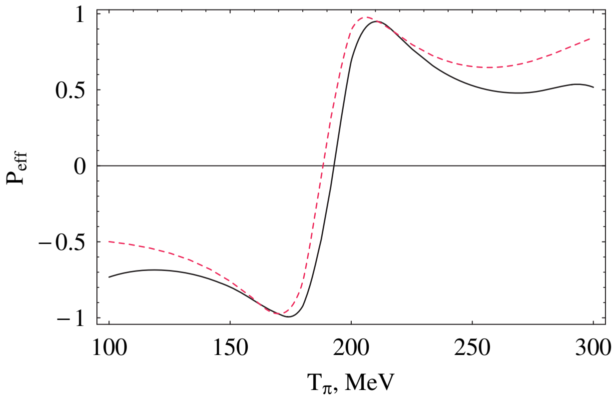

Fig. 4. DWIA calculations for the effective polarization $P_{eff}(\boldsymbol{k}_p;\boldsymbol{k}_\pi,\boldsymbol{k}_d)$ of the nuclear $1p$ proton in the reaction $^{16}\mathrm{O}(p,d\pi^+)^{15}\mathrm{N}$ under conditions (10); the dashed line shows the calculation after neglecting the real part of the optical potentials.

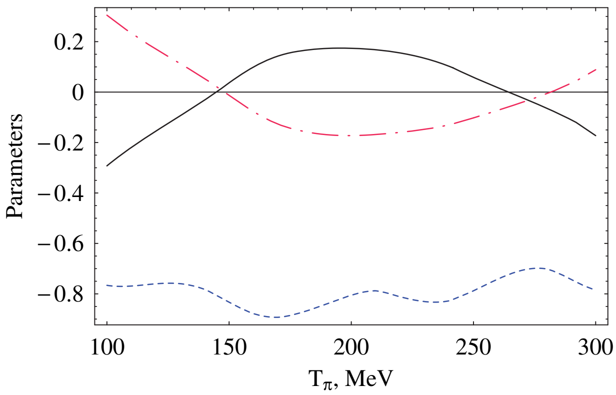

Fig. 5. Parameters A_{beam} (solid line), A_{target} (dash-dotted line) and C_{correl} (dashed line) of eqs. (13), (14) as a function of the pion energy T_π under conditions (10) of the nuclear reaction $^{16}\mathrm{O}(\boldsymbol{p},d\pi^+)^{15}\mathrm{N}$.

free two-body reaction $pp \to d\pi^+$. Their T_π-dependence under conditions (10) is presented in fig. 5.

We consider the parameters A_{beam}, A_{target} and C_{correl} in detail in sect. 4.1 in the course of extension of eqs. (13) and (14). Now note a clear correlation between the T_π-dependence of the analyzing power $\mathcal{A}_0(T_\pi)$ for the $^{16}\mathrm{O}(\boldsymbol{p},d\pi^+)^{15}\mathrm{N}(1p_{3/2}^{-1})$ reaction in fig. 2 and, on the other hand, the T_π-behavior of the effective polarization parameter P_{eff} in fig. 4.

3.4 Sensitivity of the differential cross-section of the reaction $^{16}\mathrm{O}(\mathrm{p},\mathrm{d}\pi^+)^{15}\mathrm{N}$ to the parametrization of the two-body pp $\to \mathrm{d}\pi^+$ amplitude

Since the 50s, when the reaction $pp \to d\pi^+$ was one of the hot points on the boundary between nuclear and particle physics (see, *e.g.* [16] and references herein), the problem of parametrization of its amplitude (see eq. (9) and table 1) has attracted much attention of experimentalists and theoreticians. At that time an understanding was formed about the dominant contribution of its s- and p-wave components a_0, a_1, a_2 to the multipole-spin decomposition (9). At present, it continues to serve as a key in current investigations of the problem. Detailed measurements of the angular distribution of the reaction $pp \to d\pi^+$ were performed recently in Julich with protons of energy 320 MeV [24]. They confirmed the weakness of the d-components of the amplitude at this energy. A similar conclusion was made at the Indiana University [25] where the spin transfer in the reaction $\boldsymbol{pp} \to d\pi^+$ was investigated in the proton energy range of 350–400 MeV. Experiments with higher proton energy are needed to know more about d-waves in the process under consideration. One can expect that at 500 MeV in [9] and at 650 MeV of our calculation the role of next a_3, a_4, a_5 and a_6 components of table 1 could be more pronounced in both the two-body $pp \to d\pi^+$ process and the nuclear $(p,d\pi^+)$ reaction. Our calculation of the reaction $^{16}\mathrm{O}(\boldsymbol{p},d\pi^+)^{15}\mathrm{N}$ confirms this expectation (see fig. 6).

4 Recoil nucleus and produced deuteron polarization in the reaction $^{16}\mathrm{O}(\mathrm{p},\mathrm{d}\pi^+)^{15}\mathrm{N}$

4.1 Spin density matrix of the excited recoil nucleus $^{15}\mathrm{N}(3/2^-)$

The question of polarization of the angular momentum of the excited recoil nuclei in quasi-free processes, such as the $(p,2p)$ and $(p,d\pi^+)$ reactions, could be of practical interest in triple coincidence measurements where two heavy particles (the πd pair in the latter case) are detected together with characteristic γ-radiation from the excited residual nucleus. One knows good examples of successful application of this approach to resolve the population (and possible alignment) of discrete excited states of such residual system in other studies [26,27]. In our case of the $(p,d\pi^+)$ reaction, disregard evident experimental difficulties of such measurements, we would like to have a look at possible directions of theoretical assistance in the practical realization of such measurements in the future. The approach we suggest here will be extended in the next section when discussing a similar problem of deuteron polarization.

4.1.1 Angular distribution of γ-radiation from the excited recoil nucleus

The angular distribution $W_\gamma(\theta_\gamma,\phi_\gamma)|_{\boldsymbol{k}_\pi,\boldsymbol{k}_d}$ of the γ-radiation from an excited state $|J_R\rangle$ of the recoil nucleus to the lower-lying one $|J_0\rangle$ for the reaction $^{16}\mathrm{O}(p,d\pi^+)^{15}\mathrm{N}^*(3/2^-)$, provided both momenta $\boldsymbol{k}_\pi$ and $\boldsymbol{k}_d$ of the detected pion and deuteron are known, is determined by the angular-momentum density matrix $\langle J_R M_R|\hat{\rho}_R(\boldsymbol{k}_\pi,\boldsymbol{k}_d)|J_R M_R'\rangle$ of the excited state and the intensity ratio between the $M1$ and $E2$ components of the γ-transition. The density matrix is calculated as a bilinear combination of the reaction amplitudes (2) summed

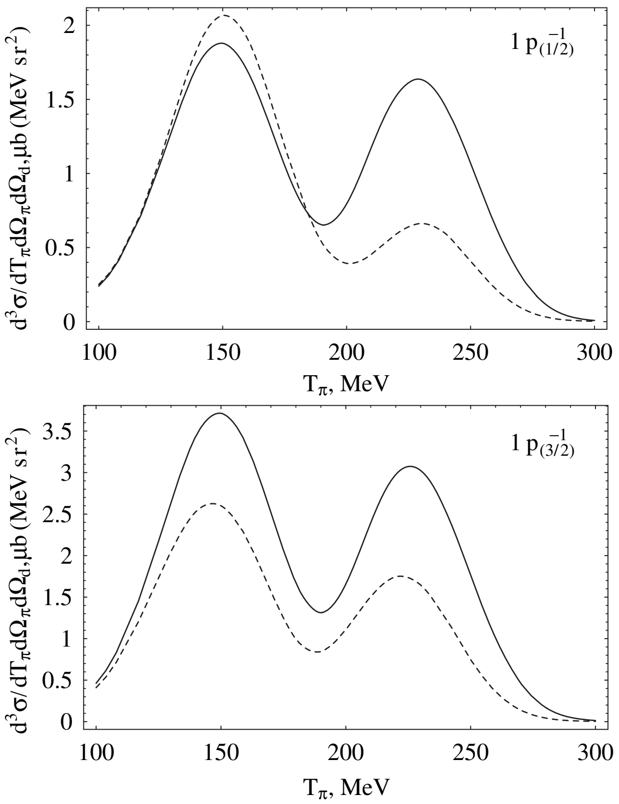

Fig. 6. Differential cross-section of the reaction $^{16}\mathrm{O}(\boldsymbol{p}, d\pi^+)^{15}\mathrm{N}$ in channels $^{16}\mathrm{O} \rightarrow {}^{15}\mathrm{N}(1p_{1/2}^{-1})$ and $^{16}\mathrm{O} \rightarrow {}^{15}\mathrm{N}(1p_{3/2}^{-1})$ calculated with the total set $a_0, \ldots, a_6$ (solid lines) and with three components a_0, a_1 and a_2 only (dashed lines) of the Bugg amplitude [10].

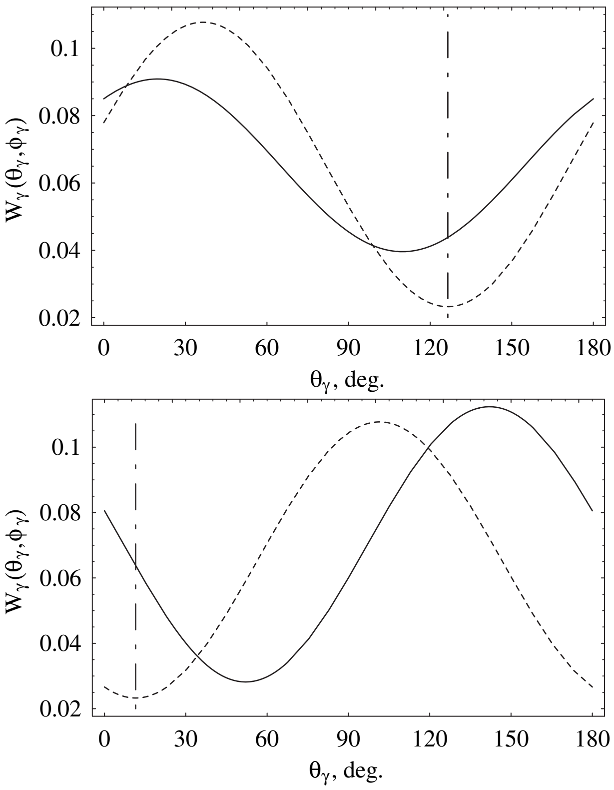

Fig. 7. Angular distribution $W_\gamma(\theta_\gamma, \phi_\gamma = 0)$ of the $^{15}\mathrm{N}^*(1p_{3/2}^{-1}) \rightarrow {}^{15}\mathrm{N}_{g.s.}(1p_{1/2}^{-1})$ γ-radiation in the reaction plane in coincidence with the deuteron and the pion from the reaction $^{16}\mathrm{O}(p, d\pi^+)^{15}\mathrm{N}$ induced by non-polarized protons under conditions (10) at a pion energy of $T_\pi = 150\,\mathrm{MeV}$ (upper part) and 190 MeV (lower part) calculated within the DWIA (solid lines) and PWIA (dashed lines) approximations. The vertical dash-dotted lines show the direction of the recoil momentum $\boldsymbol{k}_R$.

over the polarization quantum numbers of the produced deuteron

$$\langle J_R M_R|\hat{\rho}_R(\boldsymbol{k}_\pi, \boldsymbol{k}_d)|J_R M_R'\rangle = \frac{1}{2}\sum_{\mu_p,\mu_d}\langle J_R, M_R; \boldsymbol{k}_\pi, \boldsymbol{k}_d, \mu_d|\hat{F}|\boldsymbol{k}_p, \mu_p\rangle \times\langle J_R, M_R'; \boldsymbol{k}_\pi, \boldsymbol{k}_d, \mu_d|\hat{F}|\boldsymbol{k}_p, \mu_p\rangle^*. \quad (15)$$

(In a particular case of non-polarized proton beam, it is also averaged over the polarization of the incoming proton.) We parameterize such density matrix using the representation of its statistical tensors (see, *e.g.*, [28,29])

$$\rho_{kq}(J_R, J_R)|_{\boldsymbol{k}_\pi,\boldsymbol{k}_d} = \sum_{M_R,M_R'}(-1)^{J_R-M_R'} \times(J_R M_R, J_R M_R'|kq)\langle J_R M_R|\hat{\rho}_R(\boldsymbol{k}_\pi, \boldsymbol{k}_d)|J_R M_R'\rangle, \quad (16)$$

where $(J_R M_R, J_R - M_R'|kq)$ are the Clebsh-Gordan coefficients. The equation

$$W_\gamma(\theta_\gamma, \phi_\gamma)|_{\boldsymbol{k}_\pi,\boldsymbol{k}_d} = \frac{1}{4\pi} \times\left[1+\sum_k \alpha_k(J_R\rightarrow J_0)\sum_q \frac{\rho_{kq}(J_R, J_R)|_{\boldsymbol{k}_\pi,\boldsymbol{k}_d}}{\rho_{00}(J_R, J_R)|_{\boldsymbol{k}_\pi,\boldsymbol{k}_d}} Y_{kq}(\theta_\gamma, \phi_\gamma)\right] \quad (17)$$

connects angular distribution of γ-quanta with the reduced statistical tensors $A_{kq}(J_R, J_R) = \rho_{kq}(J_R, J_R)/\rho_{00}$ (*alignment parameters*) of the excited state; the numerical coefficients $\alpha_k(J_R \rightarrow J_0)$ (*radiation parameters*) are determined by the angular-momentum quantum numbers J_R and J_0 of the initial and final states of the recoil nucleus in the transition.

Figure 7 shows the considerable angular anisotropy of the 6.32 MeV γ-radiation from the $^{15}\mathrm{N}^*(1p_{3/2}^{-1}) \rightarrow {}^{15}\mathrm{N}_{g.s.}(1p_{1/2}^{-1})$ transition in the reaction $^{16}\mathrm{O}(p, d\pi^+)^{15}\mathrm{N}$ calculated within the DWIA approach under conditions (10) for the case of a non-polarized incoming proton beam; the pion energy values 150 MeV and 190 MeV correspond to the maximum and minimum in the T_π-dependence of the differential cross-section of this reaction (fig. 2). The proton, deuteron and pion interactions with the nucleus in the initial and final states of the reaction influence the angular distribution of the photon considerably and violate, in particular, its symmetry around the vector of recoil momentum $\boldsymbol{k}_R$ typical for the PWIA calculations.

Turning to the reaction $^{16}\mathrm{O}(\boldsymbol{p}, d\pi^+)^{15}\mathrm{N}^*(1p_{3/2}^{-1})$ induced by polarized protons, consider first a case when the

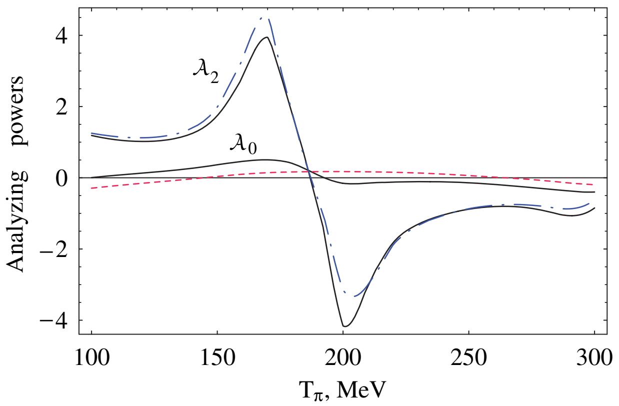

Fig. 8. Direct DWIA (solid lines) and PWIA (dashed line) calculations for the analyzing powers $\mathcal{A}_0(\boldsymbol{k}_\pi, \boldsymbol{k}_d|\boldsymbol{k}_p)$ (eq. (8)) and $\mathcal{A}_2(\boldsymbol{k}_\pi, \boldsymbol{k}_d|\boldsymbol{k}_p)$ (eq. (18)) for the reaction $^{16}\mathrm{O}(\boldsymbol{p}, d\pi^+)^{15}\mathrm{N}^*(3/2^-)$ under conditions (10). The dash-dotted line shows the DWIA calculation for $\mathcal{A}_2(\boldsymbol{k}_\pi, \boldsymbol{k}_d|\boldsymbol{k}_p)$ by eq. (20).

spin of the incoming proton is directed normally to the reaction plane. Selection rules based on general symmetry arguments cancel here all statistical tensors with the odd index q. So, to analyze the reaction $^{16}\mathrm{O}(p, d\pi^+)^{15}\mathrm{N}(3/2^-)$ one needs two sets of parameters $\rho_{k0}(3/2^-, 3/2^-; \mu_p)$ with $k = 0$ and $k = 2$, where $\mu_p = \pm 1/2$ stands for the $\boldsymbol{e}_y$-projection of the spin of the incoming proton. Two of them $\rho_{00}(3/2^-, 3/2^-; \mu_p = \pm 1/2)$ are proportional to the differential cross-section $\mathrm{d}^3\sigma_{J_R}(\boldsymbol{k}_\pi, \boldsymbol{k}_d; \boldsymbol{k}_p, \mu_p)/\mathrm{d}\Omega_\pi \mathrm{d}\Omega_d \mathrm{d}T_\pi$ of the reaction averaged over the population of the magnetic sublevels $|J_R M_R\rangle$ of the excited state. Taken together, all of them determine the angular distribution $W_\gamma(\theta_\gamma, \phi_\gamma)|_{\boldsymbol{k}_\pi, \boldsymbol{k}_d; P_y^{(in)}}$ of the radiation in the case of the $(\boldsymbol{p}, d\pi^+)$ reaction induced by protons linearly polarized along the normal to the reaction plane; $P_y^{(in)}$ stands for the polarization degree. As an indicator of the dependence of the polarization parameters $\rho_{kq}(J_R, J_R)|_{\boldsymbol{k}_\pi, \boldsymbol{k}_d, P_y^{(in)}}$ of the excited nucleus (and, hence, of the angular distribution of the radiation) on the polarization properties of the incoming beam, we introduce an *analyzing power of alignment* of the excited state of the recoil nucleus

$$\mathcal{A}_2(\boldsymbol{k}_\pi, \boldsymbol{k}_d|\boldsymbol{k}_p) = \frac{\rho_{20}(P_y^{(in)} = 1) - \rho_{20}(P_y^{(in)} = -1)}{\rho_{20}(P_y^{(in)} = 1) + \rho_{20}(P_y^{(in)} = -1)} \quad (18)$$

to refer to this ratio as to an analogue of the analyzing power of the differential cross-section of the reaction in its standard form (8).

The calculation of the analyzing powers $\mathcal{A}_2(\boldsymbol{k}_\pi, \boldsymbol{k}_d|\boldsymbol{k}_p)$ and $\mathcal{A}_0(\boldsymbol{k}_\pi, \boldsymbol{k}_d|\boldsymbol{k}_p)$ (fig. 8) shows that the alignment parameter $\rho_{20}(3/2, 3/2)$ of the recoil nucleus $^{15}\mathrm{N}^*(3/2^-)$ is more sensitive to the direction of the polarization vector of the incoming protons than the differential cross-section of the reaction. It changes also much stronger when one goes from the PWIA to the DWIA calculations. Within PWIA, both $\mathcal{A}_2(\boldsymbol{k}_\pi, \boldsymbol{k}_d|\boldsymbol{k}_p)$ and $\mathcal{A}_0(\boldsymbol{k}_\pi, \boldsymbol{k}_d|\boldsymbol{k}_p)$ are reduced

Table 2. Numerical parameters of formula (19) for the reaction $^{16}\mathrm{O}(\boldsymbol{p}, d\pi^+)^{15}\mathrm{N}^*(3/2^-)$.

k	a	b	c	d
0	1	1	1/2	1/2
2	1/2	1/2	1	1

to the parameter A_{beam} for the free two-body process:

$$\mathcal{A}_0(\boldsymbol{k}_\pi, \boldsymbol{k}_d|\boldsymbol{k}_p)|_{\mathrm{PWIA}} = \mathcal{A}_2(\boldsymbol{k}_\pi, \boldsymbol{k}_d|\boldsymbol{k}_p)|_{\mathrm{PWIA}} = A_{beam}\,.$$

4.1.2 Sensitivity of polarization characteristics of the recoil nucleus to spin-orbit forces in the proton and deuteron optical potentials

Continuing our discussion of sect. 3.2 on the role of spin-orbit effects in the distortion of the proton and deuteron wave functions in the initial and final states of the reaction, we compare direct calculations for the analyzing power $\mathcal{A}_2(\boldsymbol{k}_\pi, \boldsymbol{k}_d|\boldsymbol{k}_p)$ via the equation chain (2), (15), (16), (18) with those performed according to sect. 3.3 within the simplified concept of the effective orbital polarization of the nuclear proton. A formula was obtained in [9] representing the differential cross-section of the $(\boldsymbol{p}, d\pi^+)$ reaction via polarization parameters A_{beam}, A_{target}, C_{correl} of the free two-body process $pp \to d\pi^+$ and the nuclear effective polarization parameter P_{eff}. To illustrate the dependence of polarization characteristics of the excited state on these parameters we suggest an extension of this formula to other statistic tensors ρ_{k0}:

$$\rho_{k0}(3/2, 3/2; P_y^{(in)}) = \\ a + bA_{beam}P_y^{(in)} + cA_{target}P_{eff} + dP_y^{(in)}P_{eff}C_{correl}\,. \quad (19)$$

Here a, b, c, d are numerical parameters dependent, for a given reaction channel, only on the rank k of the statistical tensor (table 2).

The parameters A_{beam} and A_{target} for the analyzing power in the free two-body process $pp \to d\pi^+$ and the parameter C_{correl} for the proton spin correlation in this process are related to the amplitude of this process by equations

$$\tau(\mu_p, \mu'_p) = \sum_{\mu_d} |\langle \hat{K}_{\pi d}, \mu_d|\hat{t}|\hat{K}_{pp'}, \mu_p, \mu_{p'}\rangle|^2\,,$$

$$\tau_{beam}(\mu_p) = \sum_{\mu_{p'}} \tau(\mu_p, \mu_{p'}),$$

$$\tau_{target}(\mu_{p'}) = \sum_{\mu_p} \tau(\mu_p, \mu_{p'}),$$

$$A_{beam} = \frac{\tau_{beam}(1/2) - \tau_{beam}(-1/2)}{\tau_{beam}(1/2) + \tau_{beam}(-1/2)}\,,$$

$$A_{target} = \frac{\tau_{target}(1/2) - \tau_{target}(-1/2)}{\tau_{target}(1/2) + \tau_{target}(-1/2)}\,,$$

$$C_{correl} = \frac{\tau(\frac{1}{2}, \frac{1}{2}) + \tau(-\frac{1}{2}, -\frac{1}{2}) - \tau(\frac{1}{2}, -\frac{1}{2}) - \tau(-\frac{1}{2}, \frac{1}{2})}{\tau(\frac{1}{2}, \frac{1}{2}) + \tau(-\frac{1}{2}, -\frac{1}{2}) + \tau(\frac{1}{2}, -\frac{1}{2}) + \tau(-\frac{1}{2}, \frac{1}{2})}\,.$$

Using eq. (19) one can approximate the analyzing power of the differential cross-section of the reaction $^{16}\mathrm{O}(\boldsymbol{p}, d\pi^+)^{15}\mathrm{N}^*(3/2^-)$ (eq. (14)) and also, on the same level, the alignment analyzing power in this reaction

$$\mathcal{A}_2(\boldsymbol{k}_\pi, \boldsymbol{k}_d|\boldsymbol{k}_p) = \frac{A_{beam} + 2P_{eff}C_{correl}}{1 + 2P_{eff}A_{target}} \tag{20}$$

within the simplified effective orbital polarization concept and compare them with the corresponding direct calculations (8) and (18). Calculations (18) and (20) for the reaction $^{16}\mathrm{O}(\boldsymbol{p}, d\pi^+)^{15}\mathrm{N}^*(3/2^-)$ presented by solid and dash-dotted lines in fig. 8 show no considerable influence of the spin-orbit distortion of the proton and deuteron wave functions in the reaction on the alignment of the angular momentum of the excited recoil nucleus.

As was outlined in [9], the concept of effective polarization is associated with the problem of the modification of the two-body nucleon-nucleon interaction in nuclei and the localization of the reaction under consideration in nuclear matter. The calculation in fig. 3 shows that the role of such modification in the $(p, d\pi^+)$ reaction is important, indeed. However, we do not consider the concept of effective polarization as a universal one and in the next part of the paper, coming to polarization characteristics of the produced deuteron, do not address to this concept and perform our calculations starting directly from the general equations of sects. 2.1–3.1.

4.2 Vector and tensor polarization of the produced deuteron

The general character and the degree of polarization of the produced deuteron are determined by spin-dependent characteristics of the free two-body process $pp \to d\pi^+$, polarization of the incoming proton beam, kinematic and geometry conditions of detecting the pion and deuteron and also by initial-state and final-state distortions of the wave functions of the incoming and outgoing particles. Consider the polarization of the deuteron in both channels $^{16}\mathrm{O} \to {}^{15}\mathrm{N}(1p_{1/2}^{-1})$ and $^{16}\mathrm{O} \to {}^{15}\mathrm{N}(1p_{3/2}^{-1})$ of the $(p, d\pi^+)$ reaction under the same conditions (10) as in figs. 2–8 with the spin-orbit effects in the generalized distortion factors $\hat{D}_p^{(+)}(\boldsymbol{k}_p; \boldsymbol{r})$ and $\hat{D}_p^{(-)}(\boldsymbol{k}_d; \boldsymbol{r})$ taken (and, for comparison, not taken) into account.

The vector and tensor polarization of the deuteron are calculated using the statistical tensors $\rho^{(d)}_{k_d q_d}(S_d, S_d) = \rho^{(d)}_{k_d q_d}(1,1)$ of the spin of the deuteron after they are averaged over the orientation of the angular momentum $\boldsymbol{J}_R$ of the recoil nucleus. Each component of $\rho^{(d)}_{k_d q_d}(1,1)$ is a sum of two terms where the first of them does not depend on the polarization of the incoming proton (the *induced polarization*) while the other (the *transferred polarization*) is proportional to the polarization degree $P^{(in)}$ of the proton beam:

$$\rho^{(d)}_{kq}(1,1) = \left(\rho^{(d)}_{kq}\right)^{(unpol)} + \Delta\rho^{(d)}_{kq} \cdot P^{(in)};$$

$(\rho^{(d)}_{kq})^{(unpol)}$ and $\Delta\rho^{(d)}_{kq}$ are bilinear forms of the Bugg amplitudes [10].

The deuteron vector polarization in the $(\boldsymbol{p}, d\pi^+)$ reaction is calculated as

$$\boldsymbol{P}^{(d)} = \frac{\boldsymbol{P}^{(unpol)} + \sum_{ij} \boldsymbol{e}_i K_{ij} P_j^{(in)}}{1 + \boldsymbol{P}^{(in)} \cdot \boldsymbol{R}}, \tag{21}$$

where $\boldsymbol{e}_i$ with $i = x, y, z$ are unit vectors along the axes of the coordinate frame. Other parameters of this formula are calculated as *Trace* of bilinear combinations of the T-matrix of the reaction over non-observed variables of the process (in our case —over the orientation of the angular momentum of the recoil nucleus). They are

$$\boldsymbol{P}^{(unpol)} = \frac{1}{N}\,\mathrm{Tr}\left(\hat{T}^+ \boldsymbol{S}^{(d)} \hat{T}\right) \tag{22}$$

—the vector polarization of the deuteron when the incoming proton beam is non-polarized;

$$K_{ij} = \frac{1}{N}\,\mathrm{Tr}\left(S_i^{(d)} \hat{T} \sigma_j^{(p)} \hat{T}^+\right) \tag{23}$$

—the matrix of the coefficients of polarization transfer from the incoming proton to the produced deuteron. The auxiliary vector

$$\boldsymbol{R} = \frac{1}{N}\,\mathrm{Tr}\left(\hat{T} \boldsymbol{\sigma}^{(p)} \hat{T}^+\right) \tag{24}$$

is directed along the normal $\boldsymbol{e}_y$ to the reaction plane; its component R_y coincides with the analyzing power $\mathcal{A}_0(\boldsymbol{k}_\pi, \boldsymbol{k}_d|\boldsymbol{k}_p)$ of the reaction (they both vanish within the PWIA approach). The normalization factor N in the denominators of the equations above is the differential cross-section of the reaction averaged over all its polarization parameters.

4.2.1 A particular case: the incoming proton is non-polarized or polarized along the normal to the reaction plane: $\boldsymbol{P}^{(in)} = (0, P_y^{(in)}, 0)$

Under this condition the initial state of the system is symmetric relative to the reaction plane and it remains the same in the course of the reaction. Hence, the deuteron polarization vector is also perpendicular to the reaction plane: $\boldsymbol{P}^{(d)} = (0, P_y^{(d)}, 0)$. Figure 9 demonstrates a similar variation of the polarization degree $P_y^{(d)}$ with the pion energy T_π in both reaction channels $^{16}\mathrm{O} \to {}^{15}\mathrm{N}(1p_{1/2}^{-1})$ and $^{16}\mathrm{O} \to {}^{15}\mathrm{N}(1p_{3/2}^{-1})$. The magnitude $P_y^{(d)}$ of the polarization degree is very small in all three cases $P_y^{(in)} = 0; \pm 1$ in the whole range of T_π.

Turning to tensor polarization, we follow the *Madison convention* [14] to relate the degree of tensor polarization $P_{ij}^{(d)}$ of the deuteron to the statistical tensors $\rho^{(d)}_{2q}(1,1)$ of its spin, *e.g.*:

$$P_{yy}^{(d)} = \sqrt{2}\,\frac{\langle \rho^{(d)}_{20}(1,1)\rangle}{\langle \rho^{(d)}_{00}(1,1)\rangle}.$$

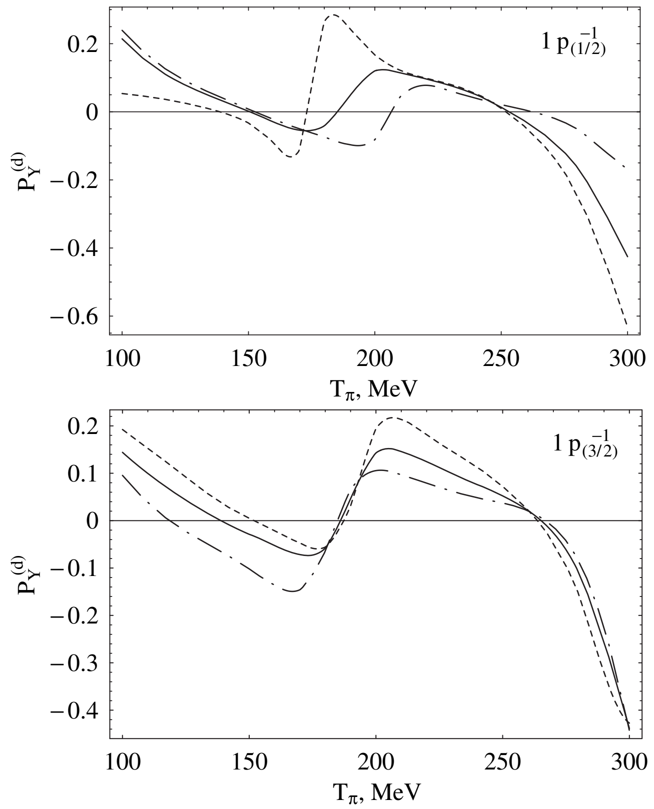

Fig. 9. Polarization degree $P^{(d)}$ of the deuteron in the reaction $^{16}O(p, d\pi^+)^{15}N$ with protons polarized along the normal to the reaction plane: $P_y^{(in)} = -1$ (dash-dotted lines); $P_y^{(in)} = 0$ (solid lines); $P_y^{(in)} = 1$ (dashed lines).

Calculations point to a considerable tensor polarization of the deuteron. Figure 10 demonstrates a strong dependence of $P_{yy}^{(d)}$ on the incoming proton polarization and an equal, in average, importance of both *transferred polarization* and *induced polarization* effects in the resulting T_π profile of $P_{yy}^{(d)}$. Solid lines in fig. 10 (top) and (center) corresponding to the case of the non-polarized proton beam show a considerable change in the magnitude and T_π behavior of the *induced* polarization of the deuteron in both the $^{16}O \to {}^{15}N(1p_{1/2}^{-1})$ and $^{16}O \to {}^{15}N(1p_{3/2}^{-1})$ channels of the nuclear reaction $^{16}O(p, d\pi^+)^{15}N$ relative to the same case in the free two-body $pp \to d\pi^+$ process. When the incoming beam is polarized, we note a strong dependence of the polarization transfer contribution to $P_{yy}^{(d)}$ on the total angular momentum $j = 1 \pm 1/2$ of the recoil nucleus ^{15}N.

4.2.2 A case when the incoming proton is polarized along its momentum: $\boldsymbol{P}^{(in)} = (0, 0, P_z^{(in)})$

Here the polarization transfer takes place in two directions: along the incoming beam (axis z) and, also in the reaction plane, normally to this direction (axis x). The scalar product $\boldsymbol{P}^{(in)} \cdot \boldsymbol{R}$ in the denominator of (21) vanishes, so this equation is reduced to

$$\boldsymbol{P}^{(d)} = \boldsymbol{e}_y P^{(unpol)} + (\boldsymbol{e}_x K_{xz} + \boldsymbol{e}_z K_{zz})\, P_z^{(in)}\,.$$

The first component of this polarization vector, normal to the reaction plane, represents the polarization induced under particle-nucleus interactions in the initial and final states of the reaction; within the PWIA approach it vanishes. Polarization transfer coefficients K_{xz} K_{zz} show the magnitude and direction of the in-plane components of $\boldsymbol{P}^{(d)}$. Figure 11 shows their dependence on the pion energy T_π in both channels of the reaction $^{16}O(\boldsymbol{p}, d\pi^+)^{15}N$.

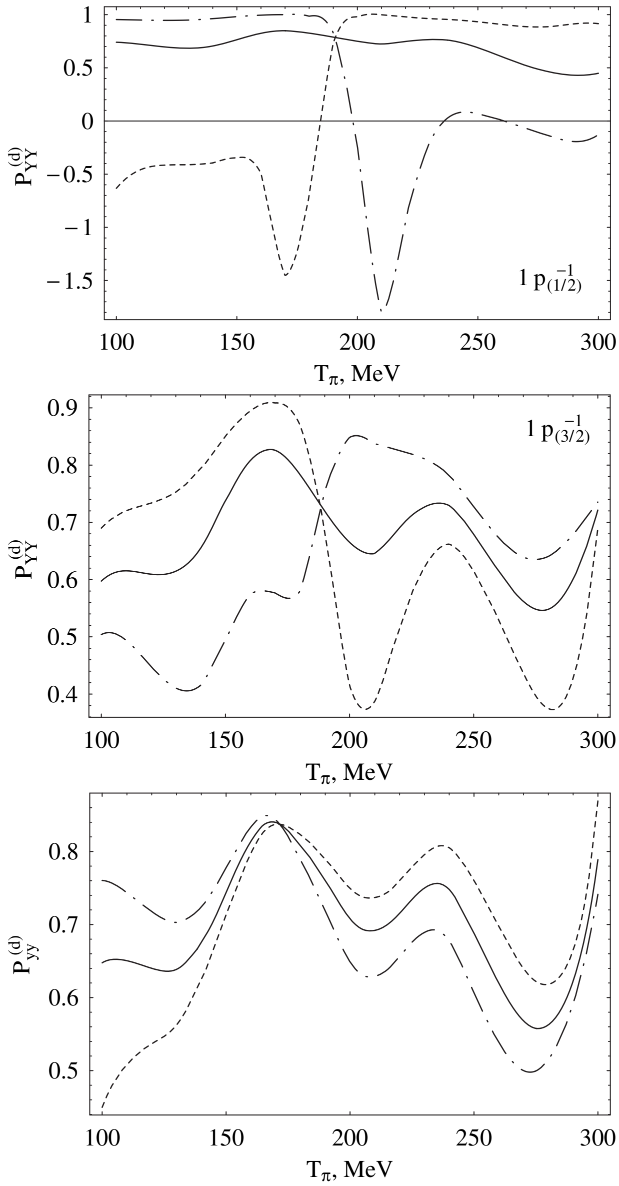

Fig. 10. Top and center: tensor polarization $P_{yy}^{(d)}$ of the deuteron in the reaction $^{16}O(\boldsymbol{p}, d\,\pi^+)^{15}N$ with protons polarized normal to the reaction plane: $P_y^{(in)} = -1$ (dash-dotted lines); $P_y^{(in)} = 0$ (solid lines); $P_y^{(in)} = 1$ (dashed lines). Bottom: the same for the free reaction $\boldsymbol{p}\,p \to d\,\pi^+$ under conditions (10) for the $(\boldsymbol{p}, d\,\pi^+)$ nuclear reaction.

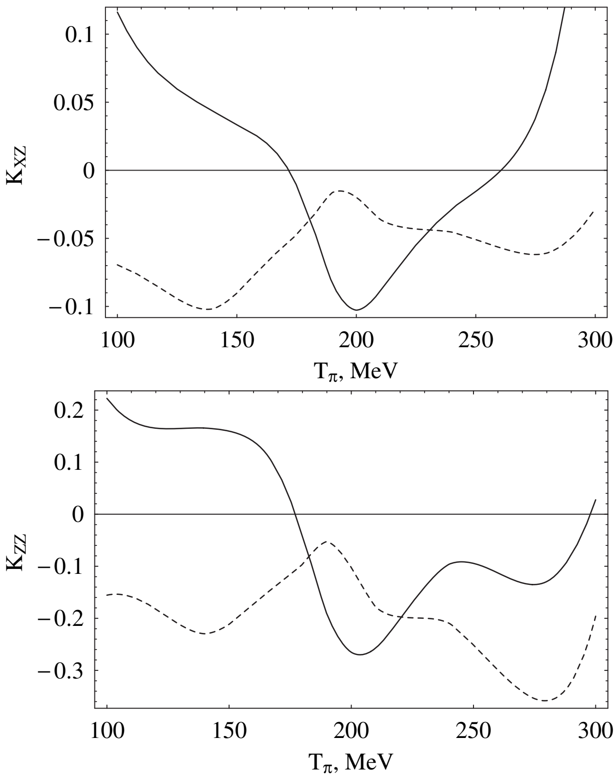

Fig. 11. Polarization transfer coefficients K_{xz} and K_{zz} for the channels $^{16}\mathrm{O} \to {}^{15}\mathrm{N}(1p^{-1}_{1/2})$ (solid lines) and $^{16}\mathrm{O} \to {}^{15}\mathrm{N}(1p^{-1}_{3/2})$ (dashed lines) of the reaction $^{16}\mathrm{O}(\boldsymbol{p}, d\pi^+)^{15}\mathrm{N}$ induced by protons polarized along their momentum.

4.2.3 Sensitivity of the deuteron polarization to the parametrization of the two-body $pp \to d\pi^+$ amplitude

Contrary to the conclusions made after $(p, d\pi^+)$ experiments with proton energy below 400 MeV [24,25], the differential cross-section of the reaction $^{16}\mathrm{O}(\boldsymbol{p}, d\pi^+)^{15}\mathrm{N}$ at our energy of 650 MeV shown in fig. 6 turned out to be clearly sensitive to the d-components a_3, a_4, a_5 and a_6 of the Bugg amplitude of the elementary two-body $p\,p \to d\pi^+$ process. To continue the discussion of this question in sect. 3.4, we look at it from the point of view of the polarization characteristics of the produced deuteron.

The top part of fig. 12 demonstrates an example related to the reaction $^{16}\mathrm{O}(\boldsymbol{p}, d\pi^+)^{15}\mathrm{N}(1p^{-1}_{3/2})$ induced by 650 MeV protons polarized along their momentum. Until the amplitudes a_3, a_4, a_5, a_6 are included in the calculation (dashed line), the z-component of the vector polarization of the deuteron retains, as a whole, the orientation of the spin of the proton (the polarization transfer coefficient K_{zz} is, on average, positive). After taking the d-amplitudes into account (solid line), a sort of inversion of the spin orientation occurs: the coefficient K_{zz} of the polarization transfer becomes negative in almost the whole range of the T_π. A rising contribution of the d-waves into the polarization transfer from the proton to the deuteron in the free two-body $pp \to d\pi^+$ process between 450 and 800 MeV (see fig. 12, bottom) is the origin of this phenomenon.

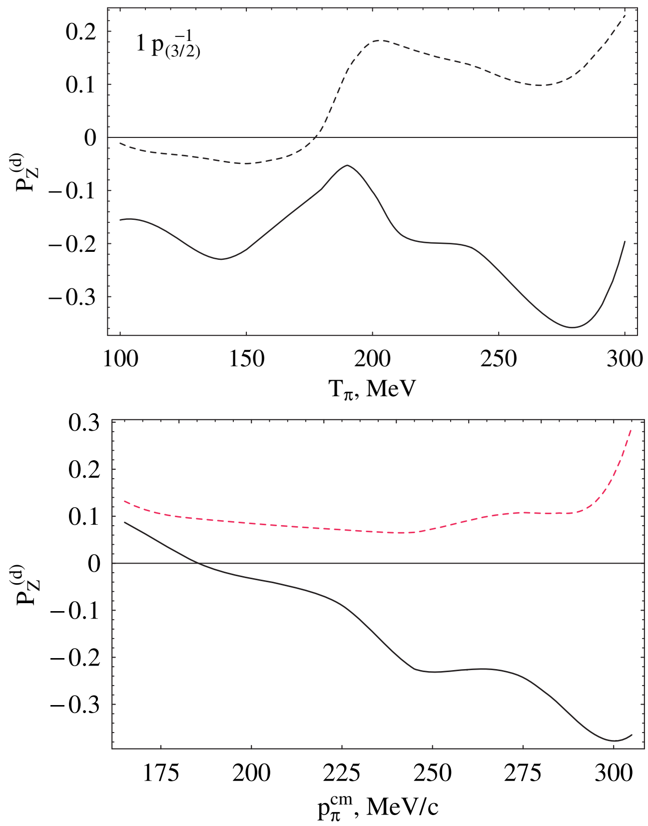

Fig. 12. Top: the component $P^{(d)}_z$ of the vector polarization of the deuteron in the reaction $^{16}\mathrm{O}(\boldsymbol{p}, d\,\pi^+)^{15}\mathrm{N}(1p^{-1}_{3/2})$ at $T_p = 650\,\mathrm{MeV}$ in the case of incoming protons totally polarized along their momentum ($P^{(in)}_z = 1$). Bottom: the same for the free reaction $\boldsymbol{p}\,p \to d\,\pi^+$ under conditions (10) for the nuclear reaction $(\boldsymbol{p}, d\,\pi^+)$. Solid lines —calculations with the total set $a_0, \ldots, a_6$ of the Bugg amplitudes [10]; dashed lines —calculations with s-wave and p-wave amplitudes a_0, a_1, a_2 only.

4.2.4 The influence of spin-orbit forces in the proton-nucleus and deuteron-nucleus optical potentials on the deuteron polarization

It was shown in sects. 3.2 and 4.1 that the sensitivity of the differential cross-section and analyzing power of the reaction $^{16}\mathrm{O}(\boldsymbol{p}, d\,\pi^+)^{15}\mathrm{N}$ as well as of the alignment analyzing power $\mathcal{A}_2(\boldsymbol{k}_\pi, \boldsymbol{k}_d|\boldsymbol{k}_p)$ for the excited $^{15}\mathrm{N}(1p^{-1}_{3/2})$ recoil nucleus to the spin-orbit particle-nucleus interactions in the initial and final states of the reaction is very small. This is not so definite for the polarization characteristics of the produced deuteron. On the contrary, fig. 13 demonstrates a strong change in the profile of the T_π-dependence of the deuteron vector polarization degree $P^{(d)}_y$ in both reaction channels $^{16}\mathrm{O} \to {}^{15}\mathrm{N}(1p^{-1}_{1/2})$ and $^{16}\mathrm{O} \to {}^{15}\mathrm{N}(1p^{-1}_{3/2})$ when the spin-orbit term is excluded from the optical potentials of proton-nucleus and deuteron-nucleus interactions. True, the magnitude of vector polarization is very small in both examples. The tensor polarization is expected to be much higher (fig. 14). Here, the spin-orbit distortion effect is weak.

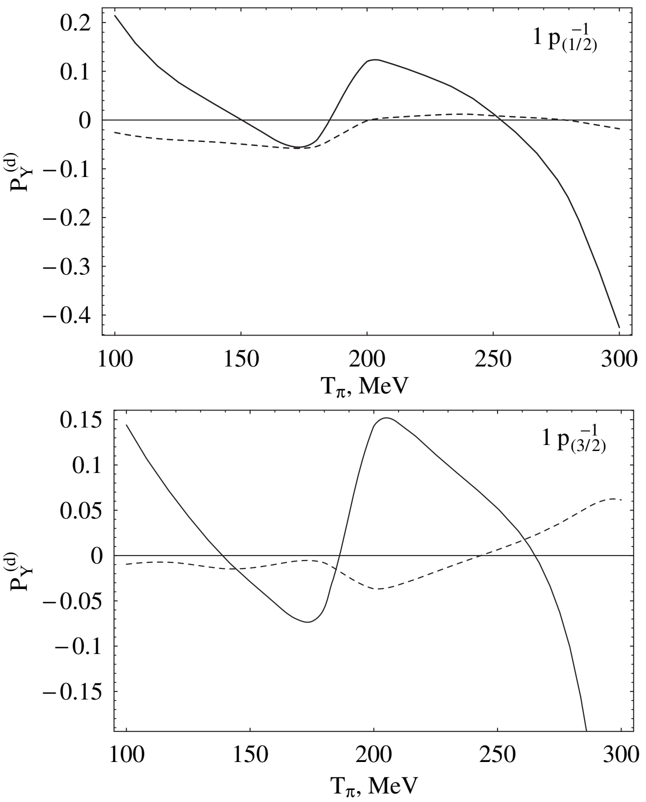

Fig. 13. Vector polarization degree $P_y^{(d)}$ of the deuteron in the reactions $^{16}\mathrm{O}(p, d\pi^+)^{15}\mathrm{N}(1p_{1/2}^{-1})$ and $^{16}\mathrm{O}(p, d\pi^+)^{15}\mathrm{N}(1p_{3/2}^{-1})$ induced by non-polarized protons; solid lines —the same as in fig. 9 ($P_y^{(in)} = 0$); dashed lines —after extracting the spin-orbit term from the proton-nucleus and deuteron-nucleus optical potentials.

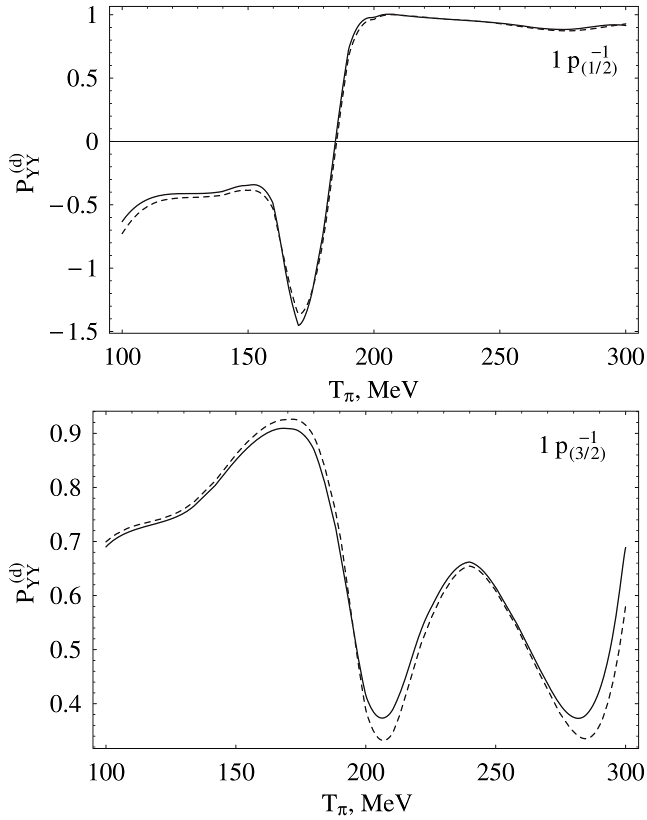

Fig. 14. Tensor polarization $P_{yy}^{(d)}$ of the deuteron in the reaction $^{16}\mathrm{O}(\boldsymbol{p}, d\pi^+)^{15}\mathrm{N}(1p_{1/2}^{-1})$ and $^{16}\mathrm{O}(\boldsymbol{p}, d\pi^+)^{15}\mathrm{N}(1p_{3/2}^{-1})$ induced by protons totally polarized along the normal to the reaction plane; solid lines —the same as in fig. 10 ($P_y^{(in)} = 1$); dashed lines —after extracting the spin-orbit term from the proton-nucleus and deuteron-nucleus optical potentials.

5 Conclusion

Coincidence measurements on the reaction $^{16}\mathrm{O}(\boldsymbol{p}, d\,\pi^+)^{15}\mathrm{N}$ with polarized protons could be, due to shell model advantages of the doubly magic target nucleus $^{16}\mathrm{O}$ against the $^{12}\mathrm{C}$ nucleus used in earlier studies, an important contribution to deeper understanding the general features of the $(p, d\,\pi^+)$ reaction as a specific sort of nuclear quasi-free processes. We suggest our DWIA calculations as a theoretical scheme for extended experiments to be performed including, besides the differential cross-section and the analyzing power $(p, d\,\pi^+)$ measurements, also the polarization characteristics of the produced deuteron and, in perspective, of the excited recoil nucleus. A proton energy of 650 MeV, higher than in earlier $(p, d\,\pi^+)$ studies, promises to be a good step to even higher energies to investigate the interrelation between various aspects of the mechanism of the reaction and those related to the nuclear structure and the initial- and final-state particle-nucleus interactions. At this energy, our calculations point to a high sensitivity of various observables of the reaction —from the differential cross-section to the polarization transfer characteristics of the reaction with polarized protons— to the spin-multipole decomposition of the amplitude of the basic two-body $pp \to d\pi^+$ process. On the other hand, both conclusions about the role of spin-dependent forces in the proton-nucleus and, especially, in the deuteron-nucleus optical potentials following out from our DWIA calculations —no sensitivity to them of the differential cross-section of the reaction and the analyzing power and, opposite to this, their well pronounced effect in the proton-to-deuteron polarization transfer— confirm the general expectations made on this point earlier [9]. Looking forward, it is worthwhile to add that our computer code elaborated in the course of the study can serve for analogous calculations in a wide range of conditions concerning target nuclei, recoil nucleus excitations, the energy and polarization characteristics of the beam, as well as kinematic and geometry conditions of the coincidence measurements.

In perspective, we consider our $(p, d\,\pi^+)$ study as a step towards the theoretical investigation of a wider class of quasi-free cluster formation nuclear reactions such as $(p, t\,\pi^+)$, $(p, {}^3\mathrm{He}\,\pi^+)$ and $(p, {}^3\mathrm{He}\,\eta)$ [30].

The participation of P.V. Safronov in the work at its earlier stage and fruitful discussions with Prof. L.S. Azhgirei are highly appreciated.

References

1. C. Ruhla, M. Riou, J.P. Garron, J.C. Jacmart, L. Massonet, Phys. Lett. **2**, 210 (1962).
2. J.Y. Grossiord *et al.*, Phys. Rev. C **15**, 843 (1977).
3. V.V. Balashov, A.N. Boyarkina, Izv. Akad. Nauk SSSR, Ser. Fiz. **28**, 359 (1964).
4. V.V. Balashov, A.N. Boyarkina, I. Rotter, Nucl. Phys. **59**, 417 (1964).
5. L.S. Azhgirei, Z.B. Krumstein *et al.*, Jad. Fiz. **13**, 6 (1971).
6. V.V. Balashov, V.I. Markov, Nucl. Phys. A **163**, 465 (1971).
7. L.S. Azhgirei, Z. Cisek *et al.*, Nucl. Phys. A **195**, 581 (1972).
8. A.A. Cowley *et al.*, Phys. Rev. C **45**, 1745 (1992).
9. M. Benjamintz *et al.*, Phys. Rev. C **58**, 964 (1998).
10. D.V. Bugg *et al.*, Nucl. Phys. A **477**, 546 (1988).
11. SAID, `http://gwdac.phys.gwu.edu/analysis/pdanalysis.html`.
12. O.V. Miklukho, N.P. Aleshin, S.L. Belostotski *et al.*, Nucl. Phys. A **683**, 145 (2001).
13. B. Van Overmeire *et al.*, Phys. Rev. C **73**, 064603 (2006).
14. H.H. Barschall, W. Haeberli (Editors), *The Madison Convention, Proceedings of the 3rd International Symposium on Polarization Phenomena in Nuclear Reactions* (The University of Wisconsin Press, Madison, 1970) p. XXV.
15. I.S. Shapiro, V.M. Kolybasov, G.R. Augst, Nucl. Phys. **61**, 353 (1965).
16. F. Mandl, T.T. Regge, Phys. Rev. **99**, 1478 (1955).
17. J.A. McNeil, J.P. Shepard, S.J. Wallace, Phys. Rev. Lett. **50**, 1439; 1443 (1983).
18. Nguyen Van Sen *et al.*, Nucl. Phys. A **464**, 717 (1987).
19. C. Garcia-Recio, E. Oset *et al.*, Nucl. Phys. A **526**, 685 (1991).
20. Particle Data Group (W.-M. Yao *et al.*), J. Phys. G **33**, 1 (2006).
21. H.C. Newns, M.Y. Refai, Proc. Phys. Soc. London, Sect. A **71**, 627 (1958).
22. J. Krein, Th.A.J. Maris, B.B. Rodrigues, E.A. Veit, Phys. Rev. C **51**, 2646 (1995).
23. N.S. Chant, P.G. Roos, Phys. Rev. C **38**, 787 (1988).
24. M. Betigeri *et al.*, Phys. Rev. C **63**, 044011 (2001).
25. B.V. Przewoski *et al.*, Phys. Rev. C **61**, 064604 (2000).
26. V.V. Balashov, V.L. Korotkikh, V.N. Mileev, Phys. Lett. B **49**, 120 (1974).
27. G. Sakhelashvili *et al.*, Phys. Rev. Lett. **95**, 033201 (2005).
28. S. Devons, L.J.B. Goldfarb, in *Handbuch der Physik*, edited by S. Flugge, Vol. **42** (Springer-Verlag, Berlin, 1957) p. 362.
29. V.V. Balashov, A.N. Grum-Grzhimailo, N.M. Kabachnik, *Polarization and Correlation Phenomena in Atomic Collisions* (Kluwer Academic/Plenum Publishers, New York, 2000).
30. V.V. Balashov, *International Nuclear Physics Conference, INPC 2004, Goeteborg, Sweden, June 27 – July 2, 2004, Book of Abstracts* (Chalmers University of Technology and Goeteborg University, 2004) p. 270.